Mol. Cells *30*, 113-119, August 31, 2010
DOI/10.1007/s10059-010-0095-y

Molecules and Cells

Characterization of SHORT-ROOT Function in the *Arabidopsis* Root Vascular System

Nan-le Yu[1], Shin Ae Lee[1,3], Mi-Hyun Lee[1,3], Jung-Ok Heo[1], Kwang Suk Chang[1,2], and Jun Lim[1,2,*]

Development of the vascular tissues is a dynamic process that integrates extrinsic and intrinsic factors to control vascular tissue formation throughout the plant life cycle. During vascular tissue formation in *Arabidopsis* roots, radial and longitudinal signals, including nuclear factors and plant hormones, control the developmental processes involved in the specification, differentiation, and maintenance of the correct cell types. SHR, a GRAS transcription factor, has been known to regulate the specification of the stem cell niche and ground tissue identity in the root meristem in a non-cell-autonomous manner. However, the role of SHR in the root vasculature is relatively overlooked, despite localization of its mRNA and protein in the stele. Here, we investigated the role of SHR in the vascular system of the primary root using a reverse genetic approach and detailed phenotypic analysis. A novel, loss-of-function null mutant, *shr-6*, was isolated in the Columbia background, and vascular patterning was characterized in detail. Our results reveal that *shr* mutants have developmental defects in both protophloem and protoxylem elements. Our study also suggests that SHR plays a central role in the root vascular system to control patterning processes, possibly regulated by longitudinal and radial signals.

INTRODUCTION

The plant vascular system serves as a continuous conduit system to transport and allocate water, ions, nutrients, and hormones, in a manner analogous to the arterial and venous systems in animals. In *Arabidopsis* roots, concentric layers of epidermis, cortex, and endodermis (outer to inner layers) encircle the stele (which consists of the pericycle and vascular system) (Fig. 1A). Stem cells in contact with an organizing center, known as the "quiescent center (QC)", a group of mitotically less active cells, can be identified in the root tip (Dolan et al., 1993; Lim and Lee, 2007). Together, the stem cells and the QC constitute a stem cell niche in the root meristem (Sabatini et al., 2003). In the center of the root is the vascular system, which is composed of two distinct tissue types: phloem and xylem. Both phloem and xylem are derived from the vascular meristem (procambium) by a series of asymmetric cell divisions (Carlsbecker and Helariutta, 2005). The phloem is composed of enucleated conducting sieve elements (SE), companion cells (CC), non-conducting parenchyma cells and fibers, whereas the xylem consists of enucleated conducting tracheary elements (TE), non-conducting parenchyma cells, and xylem fibers (Bauby et al., 2007; Baucher et al., 2007; Carlsbecker and Helariutta, 2005).

Recent molecular and genetic research has revealed the regulatory mechanisms that specify these two tissue types (Bonke et al., 2003; Dettmer et al., 2009; Mahonen et al., 2000; 2006). The first gene identified in the phloem specification, *ALTERED PHLOEM DEVELOPMENT* (*APL*), encodes a MYB transcription factor that is necessary for phloem-related asymmetric cell division and cell differentiation. In addition, APL suppresses xylem differentiation in the location where the phloem is specified (Bonke et al., 2003). Mutations in the cytokinins (CK) receptor [Arabidopsis Histidine Kinase 4 (AHK4)/CYTOKININ RESPONSE 1 (CRE1)/WOODEN LEG (WOL)] cause a dramatic decrease in the number of cell divisions in the root vasculature, and as a result, the null mutants lack phloem tissues in the root (Mahonen et al., 2000; Scheres et al., 1995). Furthermore, the triple *ahk2 ahk3 ahk4* mutants for the three genes encoding the CK receptor family (CRE family receptors; AHK2, AHK3, and AHK4) in *Arabidopsis* also exihibit a drastic reduction of cell numbers within the vascular bundle (Higuchi et al., 2004; Inoue et al., 2001; Nishimura et al., 2004). Consequently, all the vascular cell files are specified as protoxylem. Similarly, depletion of CK by ectopically expressing the *CYTOKININ OXIDASE 2* (*CKX2*) gene under the *CRE1* promoter leads all the vascular cells in the root vascular bundle to the protoxylem lineage (Werner et al., 2001). In addition, AHP6, an inhibitory pseudophosphotransfer protein essential for protoxylem specification, counteracts CK signaling in the root vasculature (Mahonen et al., 2006). These results indicate that CK signaling, possibly through the CRE-family receptors, is required for cell proliferation and maintenance of stem cell activity in procambium cells (Dettmer et al., 2009; Mahonen et al., 2000; 2006; Nishimura et al., 2004; Werner et al., 2001).

SCARECROW (SCR) and SHORT-ROOT (SHR), which belong to a plant-specific GRAS transcription factor family, regulate radial patterning in the root (Bolle, 2004; Di Laurenzio et al., 1996; Helariutta et al., 2000; Lee et al., 2008; Pysh et al., 1999). Loss of either SCR or SHR function produces roots with

[1]Department of Bioscience and Biotechnology, Konkuk University, Seoul 143-701, Korea, [2]Bio/Molecular Informatics Center, Konkuk University, Seoul 143-701, Korea, [3]These authors contributed equally to this work.
*Correspondence: jlim@konkuk.ac.kr

Received February 1, 2010; revised April 19, 2010; accepted April 22, 2010; published online July 23, 2010

Keywords: *Arabidopsis*, GRAS transcription factor, SHORT-ROOT, vascular development

Table 1. Primer sequences used in PCR analysis

Forward primer		Reverse primer	
Primer name	5′-3′	Primer name	5′-3′
AHP6-F	CGCCCAGGGTGCTTGA	AHP6-R	TCTTGAGGTAATGATACTCATGCTCTACT
APL-F	AGTCTTTCAGCAGCGGTGGG	APL-R	TGGTCGAGGACTTGGTCGGT
SCR-F	TAGCGGTTGGAGGACCATCG	SCR-R	CGCTTGTGTAGCTGCATTTCC
SHR-F	TGGTCGAGGAGGATGAGGAATAG	SHR-R	ACACTGTACCATCGACCAAACACC
GAPC-F	AGCTGCTACCTACGATG	GAPC-R	CACACGGGAACTGTAAC
VND6-F	CCCAACTACAATAATGCAACGA	VND6-R	TTGGCTCATGATTAGCTGAGAA
VND7-F	GGGACGAATAAAGATCAGAACG	VND7-R	ATGCGGATGTATGACTTGTGTC
proSHR-F	CACCGTATCGAGACAAACGAGAAAATCATGATG	proSHR-R	AAT GAA TAA GAA AAT GAA TAG AAG
Salk_002744-F	TCGTTGACAAACTTGTTGGCC	Salk_002744-R	TCCACCAAACCCATTCTCTAC
LB1	GGCAATCAGCTGTTGCCCGTCTCACTG GTG		

an aberrant ground tissue layer. In *scr* the single ground tissue exhibits mixed characteristics of the cortex and endodermis, but *shr* mutant roots lack the endodermis layer, indicating that SHR is required for the endodermis specification and that SCR is needed for the asymmetric division that separates the cortex and endodermis lineages (Benfey et al., 1993; Di Laurenzio et al., 1996; Helariutta et al., 2000). It is well established that *SHR* mRNA is transcribed and translated in the stele, and its protein moves into the adjacent cells [the endodermis, cortex/endodermis initial (CEI), cortex/endodermis initial daughter (CEID), and the QC] (Cui et al., 2007; Gallagher and Benfey, 2009; Gallagher et al., 2004; Nakajima et al., 2001). Consequently, SHR activity in the adjacent cells activates expression of *SCR*, a downstream target gene of SHR, for the specification of QC and ground tissue formation.

Despite localization of both its mRNA and protein in the stele, the role of SHR in the root vasculature has been overlooked. Here we report that *shr* mutants have developmental defects in the root vascular system other than the stem cell niche specification and ground tissue formation. In particular, *shr* mutants exhibit aberrant specification and/or patterning in both protophloem and protoxylem of the root. Our results suggest that SHR plays an important role in the development of protophloem and protoxylem elements, and it possibly is regulated by longitudinal and radial signals.

MATERIALS AND METHODS

Plant materials, growth conditions, and transformation

All lines used in this study were of *Arabidopsis thaliana* Columbia (Col-0) background. The *shr-2* mutant from Philip Benfey was described previously (Helariutta et al., 2000). The new null allele of *shr*, designated *shr-6* (SALK_002744), was obtained through the *Arabidopsis* Biological Resource Center (ABRC) (Alonso et al., 2003). For phenotypic analysis, 7-day-old seedlings of Col-0, *shr-2*, and *shr-6* were investigated. Transgenic plants with a transcriptional fusion of *pAPL::GUS* were received from Yka Helariutta (Bonke et al., 2003). The *pAPL::GUS* transgene was introduced into *shr-6* by pollination. Seeds were surface-sterilized and grown on MS agar plates, as described previously (Lee et al., 2008).

To produce *pSHR::GUS* transgenic plants the region approximately 2.0 kb upstream from the ATG start codon of *SHR* was amplified by PCR, and the amplified product was inserted into pENTR Directional TOPO™, a Gateway entry vector (Invitrogen, USA). Only an error-free insert was transferred to the pMDC162 binary vector containing the GUS marker gene (Curtis and Grossniklaus, 2003) using LR recombinase (Invitrogen, USA). Plant transformation with wild-type plants was performed by the floral-dip method according to Clough and Bent (1998). The T_1 plants resistant to hygromycin (100 mg/L) were selected, and subsequent homozygous T_2 plants were obtained through confirmation in the T_3 generation.

RNA isolation and PCR analysis

Total RNA was isolated from seedling roots using an RNeasy Plant Mini kit according to the manufacturer's instructions (Qiagen, USA). After RNA extraction we treated the samples with RQ1 RNase free-DNase (Promega, USA) to eliminate potential contamination of genomic DNA. The quality and quantity of the isolated RNA were inspected by both gel electrophoresis and spectrophotometry. The first strand cDNA was constructed with the iScript™ cDNA synthesis kit (Bio-Rad Laboratories, USA) according to the manufacturer's instructions. For both RT-PCR and qRT-PCR the *GAPC* gene was used as a housekeeping gene for the internal standard, as described by Dill et al. (2004). SYBR Green Realtime PCR Master Mix reagents (Toyobo, Japan) were used for qRT-PCR with the Mx3000P® QPCR System (Stratagene, USA). Gene-specific primers used for qRT-PCR are listed in Table 1. Each experiment was conducted at least three times with biological replicates.

GUS staining and microscopy

Histochemical staining of GUS activity was performed with 7-day-old seedlings, as previously described (Lee et al., 2008). Staining was terminated by replacing the staining solution with 70% ethanol.

To produce plastic sections the primary roots of either GUS stained-seedlings or respective genotypes were embedded in 1% agarose gel to orient the direction of sectioning. After progressing through the ethanol series (50, 70, 80, and 100% for 30 min each), the agarose gel blocks with root samples were transferred to Peel-A-Way disposable embedding molds (Polysciences, USA). Plastic resin blocks were made with Technovit 7100 according to the manufacturer's instructions (Heraeus Kulzer, Germany). Serial sections (5 μm each) were generated with an HM 355S microtome (Microm, Germany). Slides with plastic sections were stained with 0.5% toluidine blue solution and washed with distilled water. Subsequently, sections were observed, and pictures were obtained using an Axio Imager. A1 microscope equipped with an AxioCam MRc5 digital camera (Carl Zeiss, Germany).

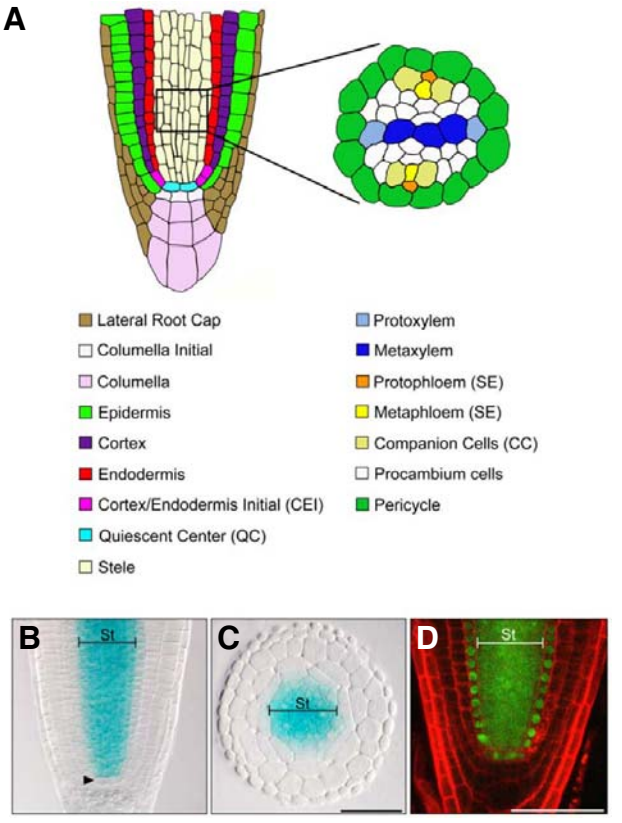

Fig. 1. Localization of mRNA and protein of *SHR* in the *Arabidopsis* root. (A) Schematic of the cellular organization of the root. (B) Longitudinal view of the transgenic *Arabidopsis* root with *pSHR::GUS* transcriptional fusion. GUS staining was detected only in cells of the stele, not in the adjacent cells. The QC is indicated with a black arrowhead. (C) The GUS staining pattern by *pSHR::GUS* in the transverse root section. No GUS staining was observed in the endodermis. (D) Confocal image of the transgenic *Arabidopsis* root with *pSHR::SHR-GFP* translational fusion. SHR-GFP was observed both in cells of the stele and in the adjacent cells. Abbreviations: St, stele. Bars = 50 μm.

Confocal images were obtained using Fluoview FV300 with a 488 nm excitation laser source (Olympus, Japan). Roots were stained with 10 mg/L propidium iodide (Sigma, USA), and mounted in distilled water.

RESULTS

Localization of mRNA and protein of the *SHR* gene in the root vascular tissues

It is known that *SHR* is expressed in the stele of the root, and its protein moves to adjacent cells to regulate the specification of the stem cell niche and the asymmetric divisions for ground tissue formation (Di Laurenzio et al., 1996; Helariutta et al., 2000; Nakajima et al., 2001). Using transgenic *Arabidopsis* plants harboring transcriptional fusion (*pSHR::GUS*) and translational fusion (*pSHR::SHR-GFP*), we verified the associated mRNA and protein localization, respectively (Figs. 1B-1D). The *cis* elements of *SHR* were used to complement *shr* mutants and have been shown to recapitulate the RNA *in situ* hybridization data (Helariutta et al., 2000; Levesque et al., 2006; Nakajima et al., 2001). Expression of *SHR* by the GUS reporter gene was

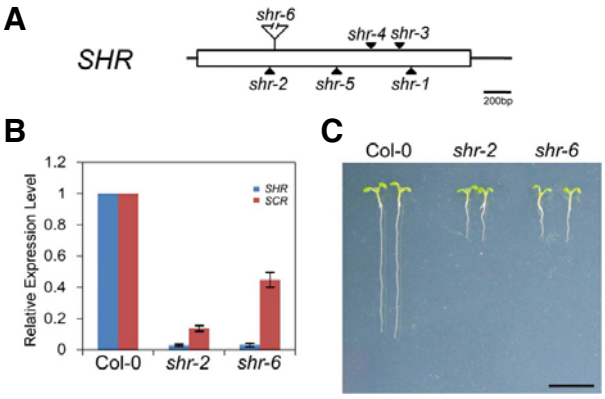

Fig. 2. Isolation of a new loss-of-function allele of the *SHR* locus. (A) The box depicts the coding region, and the lines represent the non-coding regions. The black triangles denote the position of mutations, as previously described (Benfey et al., 1993; Gallagher et al., 2004; Helariutta et al., 2000; Scheres et al., 1995). The new null mutation by a T-DNA insertion, *shr-6*, is indicated as an open triangle. (B) The transcript levels were substantially reduced in both *shr* mutants, indicating that both are null alleles. (C) Root growth of 7-day-old seedlings of Col-0 (WT), *shr-2*, and *shr-6*. Both null mutants showed precociously determinate root growth. Bar = 1 cm.

observed in all the cell files in the stele, but no expression was found in the adjacent cells (the endodermis, CEI, CEID, and the QC) (Figs. 1B and 1C). In contrast, SHR-GFP was localized in the stele and in adjacent cells, as previously reported (Gallagher et al., 2004; Helariutta et al., 2000; Nakajima et al., 2001) (Fig. 1D). Localization of both its mRNA and protein in the stele strongly suggests that SHR also regulates developmental processes in the root vascular tissues.

Identification and characterization of a novel loss-of-function allele in *SHR*

To date, five loss-of-function alleles have been reported (Benfey et al., 1993; Gallagher et al., 2004; Helariutta et al., 2000; Scheres et al., 1995). The *shr-1* and *shr-5* mutants were isolated in the Wassilewskija (Ws) background, whereas *shr-2*, *shr-3*, and *shr-4* were found in the Columbia (Col) background. Of the *shr* mutants in the Col background, *shr-3* and *shr-4* were known, unstable alleles, in which the autonomous maize En transposon disrupted the locus (Helariutta et al., 2000). To investigate the role of *SHR* in the vascular system, we isolated an additional allele in the Col background to minimize any genetic background-specific variation in morphological defects. In addition, the developmental defects of new recessive alleles in the Col background can be verified by comparing them with those of *shr-2*, the null allele in the same background. Thus, we obtained a single T-DNA insertion line, in which the *SHR* locus is disrupted, by searching the SIGnAL database (http://signal.salk.edu) (Alonso et al., 2003). Analysis of the left-border flanking sequence revealed that in the SALK_002744 line a T-DNA was inserted 418 bp from the ATG start codon, *shr-6* (Fig. 2A). To verify that it is a loss-of-function allele, we performed reverse transcription-based quantitative PCR (qRT-PCR) experiments with RNA samples extracted from the wild-type (WT), *shr-2*, and *shr-6* primary roots. Indeed, the transcript level of *SHR* was substantially low in *shr-6*, similar to that of *shr-2* (Fig. 2B). In addition, we also examined the transcript levels of *SCR*, the known direct target gene of *SHR*, in both *shr-2* and *shr-6*. As expected, expression of *SCR* also dramatically decreased

Table 2. Measurement of cell number in the stele of the primary root

Genotype	Cell No. in the stele
Col-0	31.7 ± 0.8
shr-2	10.3 ± 1.0
shr-6	11.5 ± 1.0

The number of stele cells in transverse sections (approximately 200 μm from the QC) were counted in 7-day-old seedling roots of WT, *shr-2*, and *shr-6* homozygotes. The results are displayed as the mean ± standard deviation per root.

in both mutants even though the extent of reduction of *SCR* mRNA levels varied (Fig. 2B). In addition, *shr-6* exhibited the same morphological defect as *shr-2*, in which growth of the primary root was precociously determinate (Fig. 2C). Our data indicate that *shr-6* is a null allele, like *shr-2*, in the Col background.

To define the role of *SHR* in the vascular tissues of the root we analyzed serial transverse sections of WT and *shr* primary roots along the longitudinal axis because temporal development of a cell file roughly correlates with distance from the QC (Birnbaum et al., 2003; Brady et al., 2007). In WT roots the xylem precursor cells, which are composed of five to six cell files, are localized in a row across the central region of the stele (Figs. 3A-3F). The protoxylem is located at the ends of the xylem strand adjacent to the pericycle, and the metaxylem elements are positioned between the two protoxylem elements (Baum, 2002) (Fig. 3F). However, in *shr* we found a slight - but significant - decrease in the number of cells in the xylem strand compared with that in WT (Figs. 3G-3R).

In WT roots the phloem initials, at two opposite sides, begin to form after several divisions in procambium cells. Finally, the phloem precursor cells, which are located perpendicular to the xylem strand, undergo two sets of asymmetric divisions: periclinal division and tangential division (Figs. 3B-3D). The CC files are formed by periclinal division, but cell files of SE are generated by tangential division (Bauby et al., 2007; Bonke et al., 2003) (Figs. 3B-3D). However, in *shr* phloem-related division events were markedly decreased or even absent in the stele, consequently reducing cell number in the stele (Figs. 3G-3R; Table 2). Occasionally, the aberrant cell divisions of the pericycle lineage could be observed in *shr* mutants (Fig. 3I). Together, our data suggest that SHR plays an important role in the formation of phloem and xylem elements.

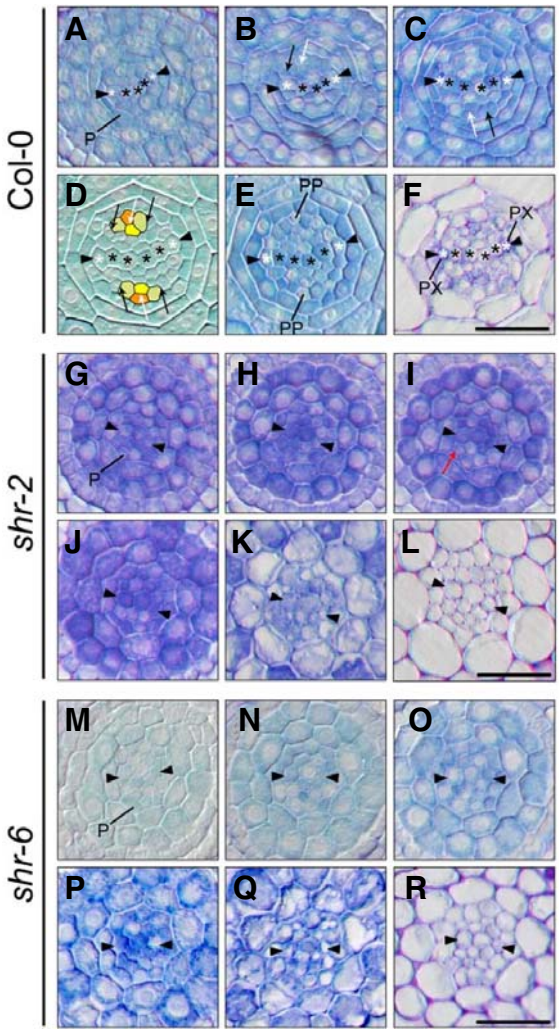

Fig. 3. Analysis of vascular tissue formation in the *Arabidopsis* primary root. Serial (5 μm thick) transverse sections of Col-0 (A-F), *shr-2* (G-L), and *shr-6* (M-R) were observed along the longitudinal axis of the root. (A) At 10 μm from the level of the QC. (B) At 20 μm from the level of the QC. Periclinal division for the companion cell (CC) lineage is indicated by black arrows, and tangential division for the sieve element (SE) lineage of the protophloem is indicated by white arrows. (C) At 40 μm from the level of the QC. (D) At 80 μm from the level of the QC. Both CC and SE cells of the phloem are pseudocolored, as shown in Fig. 1. (E) At 160 μm from the level of the QC. SE cells of the protophloem are indicated. (F) At 785 μm from the level of the QC. Arrowheads indicate the xylem strand. Asterisks depict prospective protoxylem cells (white) and prospective metaxylem cells (black). (G) At 10 μm of *shr-2*. The pericycle is indicated. (H) At 20 μm of *shr-2*. (I) At 40 μm of *shr-2*. The aberrant cell division of pericycle is indicated in red. (J) At 80 μm of *shr-2*. (K) At 160 μm of *shr-2*. (L) At 785 μm of *shr-2*. The phloem-related divisions are dramatically reduced or absent. (M) At 10 μm of *shr-6*. (N) At 20 μm of *shr-6*. (O) At 40 μm of *shr-6*. (P) At 80 μm of *shr-6*. (Q) At 160 μm of *shr-6*. (R) At 785 μm of *shr-6*. The number of cells in the vascular bundle decreased in both *shr* mutants. Abbreviations: P, pericycle; PP, SE of the protophloem; PX, protoxylem. Bars in A to R = 25 μm.

Analysis of tissue specification in the *shr* vasculature

Since the cell numbers in the vascular system are markedly reduced with the aberrant cellular organization in *shr*, we assessed the cellular organization of *shr* with cell type-specific markers. To analyze phloem specification we introduced the *pAPL::GUS* transgene into *shr*, which is normally active in the prospective SE of the protophloem (Bonke et al., 2003). In WT plants two arrays of SE files of the protophloem, which are specified at opposite sides, perpendicular to the xylem strand, clearly displayed GUS activity (100%; 35 of 35) (Figs. 4A and 4C). In contrast, the SE of the *shr* primary root frequently lacked this symmetry, resulting in a single array of the SE (68%; 17 of 25) (Figs. 4B and 4D). Occasionally, expression of *pAPL::GUS* was observed ectopically in subepidermal cells with discontinuous patches (Supplementary Fig. S1). It is currently unclear why *pAPL::GUS* expression is detected ectopically in the subepidermal cells. In addition, GUS activity in the SE of the *shr* protophloem was first detected in the elongation zone, whereas GUS staining in WT was clearly observed in the meristematic zone (Figs. 4A, and 4B). Our qRT-PCR analysis also revealed that the transcript levels of *APL* in *shr* mutants were reduced to

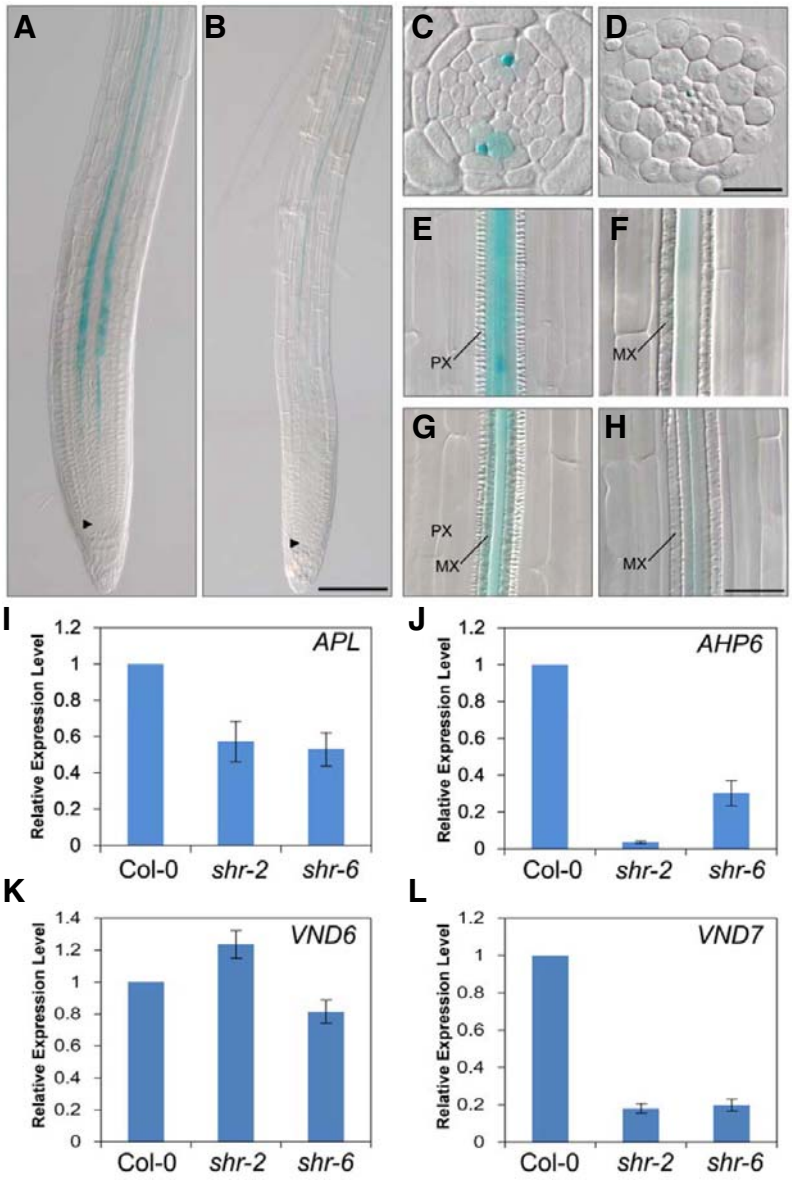

Fig. 4. Cell fate specification in the root vascular tissues. (A) The expression pattern of *pAPL::GUS* in Col-0. Two arrays of SE cell files of the protophloem were clearly observed. Blue staining was obviously detected primarily in the meristematic zone. (B) The expression pattern of *pAPL::GUS* in *shr-6*. Only a single array of SE of the protophloem was observed in the elongation zone. (C) SE cell files of the protophloem at opposite positions were marked by GUS blue staining. (D) Reduction of blue staining was visible in only one side of the prospective SE of the protophloem. Longitudinal differential interference contrast (DIC) images of Col-0 (E, G) and *shr-6* (F, H). (E) Annular cell wall thickening of the protoxylem vessels in Col-0. (F) No annular cell wall thickening of the protoxylem vessels was observed in *shr-6*. (G) Reticulated cell wall thickening of the metaxylem vessels in the maturation zone. (H) Only reticulated cell wall thickening of the metaxylem vessels was found in *shr-6*. Quantitative RT-PCR with vascular-specific markers (I-L). (I) *APL* expression for SE cells of the protophloem was reduced in *shr* mutants. (J) Expression of *AHP6* for the protoxylem and associated pericycle cells was substantially reduced in *shr* mutants. (K) *shr* mutants showed more or less similar expression of the metaxylem-specific *VND6* compared with that of the wild-type. (L) The protoxylem-specific *VND7* expression was significantly reduced in *shr* mutants. Abbreviations: PX, protoxylem; MX, metaxylem. Bars in A and B = 100 μm, and bars in C to H = 25 μm.

approximately one half of the level in WT (Fig. 4I). Our data suggest that SHR plays a key role in the specification and/or patterning of protophloem in the root vasculature in a non-cell-autonomous manner.

In WT the protoxylem positioned at the outermost ends of the xylem axis exhibits predominantly annular and spiral cell wall thickenings, whereas the metaxylem elements located between the protoxylem cells differentiate later with reticulated and pitted cell wall thickenings (Kubo et al., 2005; Mahonen et al., 2000) (Figs. 4E and 4G). In contrast, the xylem strand of the *shr* primary root consists solely of metaxylem (Figs. 4F and 4H). We also examined the xylem tissues in the maturation zone along the longitudinal axis. In WT both the protoxylem and metaxylem clearly displayed stereotyped structures, whereas in the *shr* primary root no protoxylem was seen - even in the mature region (Figs. 4G and 4H). Interestingly, metaxylem elements in *shr* occasionally were found to be discontinuous along the longitudinal axis (Supplementary Fig. S2). In addition, we analyzed the transcript levels of *AHP6*, which is expressed specifically in developing protoxylem and in associated pericycle cells (Mahonen et al., 2006). In *shr* mutants the expression of *AHP6* substantially decreased (Fig. 4J), suggesting that SHR regulates the specification of the protoxylem fate of the root vasculature. We also investigated the transcript levels of *VASCULAR-RELATED NAC-DOMAIN 6* (*VND6*) and *VND7*, which are known to regulate the developmental processes for metaxylem and protoxylem specification, respectively (Kubo et al., 2005). In *shr* mutants the expression of *VND7* dramatically decreased (Fig. 4L), but the *VND6* transcript levels were more or less similar to those of the wild-type (Fig. 4K), further corroborating the belief that SHR specifically regulates the specification of protoxylem, not metaxylem. Taken together, our data strongly suggest that SHR controls the specification and/or patterning of both protophloem and protoxylem in the root vascular system, possibly in a non-cell-autonomous manner.

DISCUSSION

The development of the vascular tissues is a dynamic process

integrating extrinsic and intrinsic factors throughout the plant life cycle. It is believed that the interplay between longitudinal and radial signals controls the spatiotemporal cell fate of vascular tissues in the root (Truernit et al., 2008). In particular, longitudinal signals regulate the timing of cell specification and/or differentiation, providing vascular network continuity, and radial signals control the developmental processes that give rise to specific cell types of the vascular cylinder in a position-dependent manner (Dettmer et al., 2009; Truernit et al., 2008).

The GRAS transcription factors SHR and SCR are key regulators in the specification of the stem cell niche and the determination of ground tissue identity of the root meristem (Benfey et al., 1993; Di Laurenzio et al., 1996; Helariutta et al., 2000). In particular, SHR protein moves to the adjacent cells from the stele to control developmental processes in a non-cell-autonomous manner (Cui et al., 2007; Gallagher and Benfey, 2009; Gallagher et al., 2004; Helariutta et al., 2000; Nakajima et al., 2001). However, the role of SHR in the root stele has been poorly characterized even though its mRNA and protein are localized in vascular tissues. Hence, in this study we attempted to provide a more detailed characterization of loss-of-function *shr* mutants, focusing on the developmental processes of the root vascular system. Intriguingly, recessive *shr* mutants displayed the aberrant cellular organization of the vascular bundle. In particular, the protophloem cell lineage of *shr* mutants is reduced to a single file in the elongation zone, visualized with *pAPL::GUS* fusion, indicating developmental defects in specification and/or patterning of protophloem. Previous studies demonstrated that native *SHR* transcripts were not detected in the phloem and adjacent pericycle cells (Gallagher et al., 2004; Sena et al., 2004). Thus, it appears that SHR also acts non-cell-autonomously to control specification and/or patterning of the protophloem cell lineage. Furthermore, the vascular cylinder of *shr* lacks protoxylem cells, suggesting the possibility that radial signals control protoxylem specification in the xylem strand. A recent study suggests that CK signaling regulates cell fate of the protoxylem associated with the pericycle cells (Mahonen et al., 2006). It is therefore tempting to speculate that CK, probably together with another plant hormone, auxin, defines the boundary of cell types in the vascular system, as suggested in the maize stele (Saleem et al., 2010), even though previous work demonstrated that the SHR pathway is independent of the CK signaling pathway (Scheres et al., 1995).

In conclusion, we have demonstrated that SHR functions non-cell-autonomously in both protophloem and protoxylem in the root vascular system. Our results suggest that SHR plays a key role in the root vascular development, possibly regulated by longitudinal and radial signals along the axis of the root.

Note: Supplementary information is available on the Molecules and Cells website (www.molcells.org).

ACKNOWLEDGMENTS

We thank the members of the Lim laboratory for useful discussions. We are also grateful to Philip Benfey and Yka Helariutta for providing plant materials. K.S. Chang was supported by a grant (2006-005-J03401). This research was supported by a grant from the National Research Foundation (NRF2010-0015691).

REFERENCES

Alonso, J., Stepanova, A., Leisse, T., Kim, C., Chen, H., Shinn, P., Stevenson, D., Zimmerman, J., Barajas, P., Cheuk, R., et al. (2003). Genome-wide insertional mutagenesis of *Arabidopsis thaliana*. Science *301*, 653-657.

Bauby, H., Divol, F., Truernit, E., Grandjean, O., and Palauqui, J.C. (2007). Protophloem differentiation in early *Arabidopsis thaliana* development. Plant Cell Physiol. *48*, 97-109.

Baucher, M., El Jaziri, M., and Vandeputte, O. (2007). From primary to secondary growth: origin and development of the vascular system. J. Exp. Bot. *58*, 3485-3501.

Baum, S.F., Dubrovsky, J.G., and Rost, T.L. (2002). Apical organization and maturation of the cortex and vascular cylinder in *Arabidopsis thaliana* (Brassicaceae) roots. Am. J. Bot. *89*, 908-920.

Benfey, P.N., Linstead, P.J., Roberts, K., Schiefelbein, J.W., Hauser, M.T., and Aeschbacher, R.A. (1993). Root development in *Arabidopsis*: four mutants with dramatically altered root morphogenesis. Development *119*, 57-70.

Birnbaum, K., Shasha, D.E., Wang, J.Y., Jung, J.W., Lambert, G.M., Galbraith, D.W., and Benfey, P.N. (2003). A gene expression map of the *Arabidopsis* root. Science *302*, 1956-1960.

Bolle, C. (2004). The role of GRAS proteins in plant signal transduction and development. Planta *218*, 683-692.

Bonke, M., Thitamadee, S., Mahonen, A.P., Hauser, M.T., and Helariutta, Y. (2003). APL regulates vascular tissue identity in *Arabidopsis*. Nature *426*, 181-186.

Brady, S.M., Orlando, D.A., Lee, J.Y., Wang, J.Y., Koch, J., Dinneny, J.R., Mace, D., Ohler, U., and Benfey, P.N. (2007). A high-resolution root spatiotemporal map reveals dominant expression patterns. Science *318*, 801-806.

Carlsbecker, A., and Helariutta, Y. (2005). Phloem and xylem specification: pieces of the puzzle emerge. Curr. Opin. Plant Biol. *8*, 512-517.

Clough, S., and Bent, A. (1998). Floral dip: a simplified method for Agrobacterium-mediated transformation of *Arabidopsis thaliana*. Plant J. *16*, 735-743.

Cui, H., Levesque, M.P., Vernoux, T., Jung, J.W., Paquette, A.J., Gallagher, K.L., Wang, J.Y., Blilou, I., Scheres, B., and Benfey, P.N. (2007). An evolutionarily conserved mechanism delimiting SHR movement defines a single layer of endodermis in plants. Science *316*, 421-425.

Curtis, M., and Grossniklaus, U. (2003). A gateway cloning vector set for high-throughput functional analysis of genes *in planta*. Plant Physiol. *133*, 462-469.

Dettmer, J., Elo, A., and Helariutta, Y. (2009). Hormone interactions during vascular development. Plant Mol. Biol. *69*, 347-360.

Di Laurenzio, L., Wysocka-Diller, J., Malamy, J., Pysh, L., Helariutta, Y., Freshour, G., Hahn, M., Feldman, K., and Benfey, P. (1996). The *SCARECROW* gene regulates an asymmetric cell division that is essential for generating the radial organization of the *Arabidopsis* root. Cell *86*, 423-433.

Dill, A., Thomas, S.G., Hu, J., Steber, C.M., and Sun, T.P. (2004). The Arabidopsis F-box protein SLEEPY1 targets gibberellin signaling repressors for gibberellin-induced degradation. Plant Cell *16*, 1392-1405.

Dolan, L., Janmaat, K., Willemsen, V., Linstead, P., Poethig, S., Roberts, K., and Scheres, B. (1993). Cellular organization of the *Arabidopsis thaliana* root. Development *119*, 71-84.

Gallagher, K.L., and Benfey, P.N. (2009). Both the conserved GRAS domain and nuclear localization are required for SHORT-ROOT movement. Plant J. *57*, 785-797.

Gallagher, K.L., Paquette, A.J., Nakajima, K., and Benfey, P.N. (2004). Mechanisms regulating SHORT-ROOT intercellular movement. Curr. Biol. *14*, 1847-1851.

Helariutta, Y., Fukaki, H., Wysocka-Diller, J., Nakajima, K., Jung, J., Sena, G., Hauser, M., and Benfey, P. (2000). The *SHORT-ROOT* gene controls radial patterning of the *Arabidopsis* root through radial signaling. Cell *101*, 555-567.

Higuchi, M., Pischke, M.S., Mahonen, A.P., Miyawaki, K., Hashimoto, Y., Seki, M., Kobayashi, M., Shinozaki, K., Kato, T., Tabata, S., et al. (2004). *In planta* functions of the *Arabidopsis* cytokinin receptor family. Proc. Natl. Acad. Sci. USA *101*, 8821-8826.

Inoue, T., Higuchi, M., Hashimoto, Y., Seki, M., Kobayashi, M., Kato, T., Tabata, S., Shinozaki, K., and Kakimoto, T. (2001). Identification of CRE1 as a cytokinin receptor from *Arabidopsis*. Nature *409*, 1060-1063.

Kubo, M., Udagawa, M., Nishikubo, N., Horiguchi, G., Yamaguchi, M., Ito, J., Mimura, T., Fukuda, H., and Demura, T. (2005). Transcription switches for protoxylem and metaxylem vessel formation. Genes Dev. *19*, 1855-1860.

Lee, M.H., Kim, B., Song, S.K., Heo, J.O., Yu, N.I., Lee, S.A., Kim, M., Kim, D.G., Sohn, S.O., Lim, C.E., et al. (2008). Large-scale analysis of the GRAS gene family in *Arabidopsis thaliana*. Plant

Mol. Biol. *67*, 659-670.
Levesque, M.P., Vernoux, T., Busch, W., Cui, H., Wang, J.Y., Blilou, I., Hassan, H., Nakajima, K., Matsumoto, N., Lohmann, J.U., et al. (2006). Whole-genome analysis of the SHORT-ROOT developmental pathway in *Arabidopsis*. PLoS Biol. *4*, e143.
Lim, J., and Lee, M.M. (2007). Root development in *Arabidopsis thaliana*: attraction from underground. J. Plant Biol. *50*, 306-314.
Mahonen, A.P., Bonke, M., Kauppinen, L., Riikonen, M., Benfey, P.N., and Helariutta, Y. (2000). A novel two-component hybrid molecule regulates vascular morphogenesis of the *Arabidopsis* root. Genes Dev. *14*, 2938-2943.
Mahonen, A.P., Bishopp, A., Higuchi, M., Nieminen, K.M., Kinoshita, K., Tormakangas, K., Ikeda, Y., Oka, A., Kakimoto, T., and Helariutta, Y. (2006). Cytokinin signaling and its inhibitor AHP6 regulate cell fate during vascular development. Science *311*, 94-98.
Nakajima, K., Sena, G., Nawy, T., and Benfey, P.N. (2001). Intercellular movement of the putative transcription factor SHR in root patterning. Nature *413*, 307-311.
Nishimura, C., Ohashi, Y., Sato, S., Kato, T., Tabata, S., and Ueguchi, C. (2004). Histidine kinase homologs that act as cytokinin receptors possess overlapping functions in the regulation of shoot and root growth in *Arabidopsis*. Plant Cell *16*, 1365-1377.
Pysh, L., Wysocka-Diller, J., Camilleri, C., Bouchez, D., and Benfey, P. (1999). The GRAS gene family in *Arabidopsis*: sequence characterization and basic expression analysis of the *SCARECROW-LIKE* genes. Plant J. *18*, 111-119.
Sabatini, S., Heidstra, R., Wildwater, M., and Scheres, B. (2003). SCARECROW is involved in positioning the stem cell niche in the *Arabidopsis* root meristem. Genes Dev. *17*, 354-358.
Saleem, M., Lamkemeyer, T., Schutzenmeister, A., Madlung, J., Sakai, H., Piepho, H.P., Nordheim, A., and Hochholdinger, F. (2010). Specification of cortical parenchyma and stele of maize primary roots by asymmetric levels of auxin, cytokinin, and cytokinin-regulated proteins. Plant Physiol. *152*, 4-18.
Scheres, B., Di Laurenzio, L., Willemsen, V., Hauser, M.T., Janmaat, K., Weisbeek, P., and Benfey, P.N. (1995). Mutations affecting the radial organisation of the *Arabidopsis* root display specific defects throughout the embryonic axis. Development *121*, 53-62.
Sena, G., Jung, J.W., and Benfey, P.N. (2004). A broad competence to respond to SHORT ROOT revealed by tissue-specific ectopic expression. Development *131*, 2817-2826.
Truernit, E., Bauby, H., Dubreucq, B., Grandjean, O., Runions, J., Barthelemy, J., and Palauqui, J.C. (2008). High-resolution whole-mount imaging of three-dimensional tissue organization and gene expression enables the study of phloem development and structure in *Arabidopsis*. Plant Cell *20*, 1494-1503.
Werner, T., Motyka, V., Strnad, M., and Schmulling, T. (2001). Regulation of plant growth by cytokinin. Proc. Natl. Acad. Sci. USA *98*, 10487-10492.